



Environmentally Friendly and Cost-Effective Gamma Shielding Based on Waste CRT Screen Glasses

Khadijah Mohammadsaleh Katubi¹ · Fatimah Mohammed A. Alzahrani¹ · Canel Eke² · Z. A. Alrowaili³ · Fatih Çalışkan⁴ · I. O. Olariño⁵ · M. S. Al-Buriahi⁶

Received: 19 July 2023 / Accepted: 12 January 2024 / Published online: 20 February 2024
© The Minerals, Metals & Materials Society 2024

Abstract

In this paper, the gamma radiation shielding properties of S-TV/TiX glasses are investigated at different photon energies using data from FLUKA simulations and the XCOM library. Three samples of TV screen glass (S-TV) doped with TiO₂ were prepared using cold isostatic pressing. The samples were designated as S-TV, S-TV/Ti10, and S-TV/Ti20 for TiO₂ concentrations of 0 wt.%, 10 wt.%, and 20 wt.%, respectively. The gamma radiation transmission data for the samples obtained from FLUKA simulations and the XCOM database were used to compute the mass attenuation coefficient (μ/ρ) of the S-TV/TiX samples. Other photon interaction parameters, including the half-value layer (HVL), mean free path (λ), effective atomic number (Z_{eff}), electron density (N_{eff}), specific gamma constants (Γ), dose rate (D_r), equivalent atomic number (Z_{eq}), exposure (EBF), and energy absorption (EABF) buildup factors were calculated from the μ/ρ data based on standard expressions and procedures. The μ/ρ values were in the range of 0.02442–12.57505 cm²/g, 0.02438–13.54632 cm²/g, and 0.02434–14.50959 cm²/g for S-TV, S-TV/Ti10, and S-TV/Ti20, respectively. Based on the obtained HVLs, it was observed that as the TiO₂ content increased, the glass thickness required to attenuate photons also increased. Analysis of the effective atomic number and electron density showed that the glass sample with lower TiO₂ content exhibited more electron interaction and hence absorbed more photons. The photon scattering potential of the glasses varied with glass composition and gamma energy. The study further showed that the trend of photon scattering ability among the glasses fluctuated at different energies. However, at 1.5 MeV, the glasses with lower TiO₂ content exhibited higher photon buildup factors. In comparison with standard radiation shielding materials such as concrete and glasses, TiO₂-doped S-TV glasses have better gamma absorption capacity and are therefore suitable for gamma-shielding applications, especially for low (keV) energies.

Keywords Glass material · gamma absorber · CRT waste · radiation shielding · eco-friendly applications

Introduction

With the rapid depletion of natural resources and the rising volume of industrial solid waste, recycling has become a crucial environmental concern. One material that has generated considerable interest with respect to recycling is glass, due to its diverse applications and waste resulting from production processes, damage, installation, and end-of-use. In many affluent nations, systematic community schemes for glass recycling and collection have already been put into place.

Researchers have recently developed glasses with a variety of components and are studying their various properties. One of these properties is shielding against different types of radiation. For example, Albarzan et al.¹ investigated how titanium dioxide (TiO₂) affects the attenuation

✉ M. S. Al-Buriahi
mohammed.al-buriahi@ogr.sakarya.edu.tr

¹ Department of Chemistry, College of Science, Princess Nourah bint Abdulrahman University, P.O. Box 84428, 11671 Riyadh, Saudi Arabia

² Department of Mathematics and Science Education, Faculty of Education, Akdeniz University, 07058 Antalya, Turkey

³ Department of Physics, College of Science, Jouf University, P.O. Box 2014, Sakaka, Saudi Arabia

⁴ Department of Metallurgical and Material Engineering, Faculty of Technology, Sakarya University of Applied Sciences, Sakarya, Turkey

⁵ Department of Physics, School of Physical Sciences, Federal University of Technology, Minna, Nigeria

⁶ Department of Physics, Sakarya University, Sakarya, Turkey

features of $\text{Na}_2\text{O}-\text{CaO}-\text{SiO}_2-\text{TiO}_2$ silicate-based glasses. Using the simulation of gamma transmission in a narrow-beam geometry and standard theoretical methods, they reported that the addition of TiO_2 content in the glasses increased the elastic modulus and radiation shielding characteristics. Kebaili et al.² investigated the effect of replacing TiO_2 with V_2O_5 on the optical and radiation shielding features of $\text{Li}_2\text{O}-\text{B}_2\text{O}_3-\text{ZnO}-\text{TiO}_2-\text{V}_2\text{O}_5$ glasses using theoretical and simulation methods. They noted that replacing TiO_2 with V_2O_5 had a significant effect on the radiation shielding features but a small effect on the optical properties of the glasses. Singh et al.³ theoretically examined the effect of TiO_2 content on the radiation shielding ability of $\text{TiO}_2-\text{CeO}_2-\text{PbO}-\text{B}_2\text{O}_3$ glasses. Tungsten oxide-doped tellurium and titanium glasses were studied using theoretical-simulation methods by Hussan et al.,⁴ and their findings revealed that the addition of WO_3 has a positive effect on shielding against fast neutrons. Karami et al.⁵ investigated the radiation shielding properties of $\text{TeO}_2-\text{Na}_2\text{O}-\text{BaO}-\text{TiO}_2$ alloyed glasses using a theoretical-simulation method, and found that TNB-Ti15, which possessed the highest content of TiO_2 , demonstrated the best radiation shielding capability. Arvaneh et al.⁶ investigated the effects of TiO_2 on the radiation shielding ability of $\text{Bi}_2\text{O}_3-\text{ZnO}-\text{Pb}_3\text{O}_4-\text{Al}_2\text{O}_3$ glasses using theoretical and simulation techniques, and reported that as TiO_2 content increased, the mass attenuation coefficient of the glasses increased, whereas the effective atomic numbers decreased. Es-soufi et al.⁷ examined the effect of TiO_2 on the radiation shielding properties of $\text{Na}_2\text{O}-\text{Na}_2\text{WO}_4-\text{P}_2\text{O}_5:\text{TiO}_2$ tungsten-based glasses using theoretical methods. Their results showed that the addition of TiO_2 had a significant effect, especially at low energies, and the half-value layer (HVL) of the glasses increased with increasing TiO_2 content. Rahmat et al.⁸ experimentally studied the x-ray shielding properties of composite cement, TiO_2 , and barium carbonate (BaCO_3), and they compared their results with theoretical results. Their results indicated that the $\text{TiO}_2/\text{BaCO}_3$ composite had the smallest HVL and mean free path, whereas it has the greatest linear attenuation coefficient in the studied glasses.

Discarded, damaged, or out-of-use cathode ray tube (CRT) glass from TVs and computer monitors has been recognized as a good radiation shielding material in pristine form or as an admixture in other glass, ceramics, or concrete composites.^{9–15} The high gamma radiation potential of CRT glass has been linked to its high density and the presence of dense atoms such as Ba, Pb, Sb, and Sr.^{14,15} These dense atoms have high atomic numbers and, consequently, a high probability of interaction with gamma photons and charged radiation. Pristine CRT glass and composite materials containing CRT glass have thus been recognized as effective radiation shields with practical applications in hospitals and other nuclear facilities. The presence of Pb, especially in the

cone part of the CRT glass, makes it a toxic material, and thus its use can be hazardous to humans and the environment as a result of the risk of Pb leaching. However, researchers have confirmed that to avoid Pb poisoning through leaching from CRT glasses, the screen section of the glass could be used in pristine form or as an admixture in composite materials intended for shielding. It was found that the screen glass is also dense and contains high-atomic-number atoms such as Ba, Sr, and Zr; therefore, its shielding performance could also be appreciable.^{14,15} Recently, Buriahi et al.¹⁵ compared the radiation shielding parameters of cone (CCRT) and screen (PCRT) glasses from a CRT obtained from an out-of-use CRT. They showed that PCRT glass had higher gamma-ray, charged particle (carbon ions, alpha particles, protons, and electrons), thermal, and fast neutron transmission performance than CCRT glass. The study showed that although PCRT glass was inferior to CCRT glass with respect to radiation attenuation, its radiation absorption efficiency was better than some concrete shields and commercial shielding glasses. The shielding ability of screen glasses from CRT can be enhanced when mixed with materials with high radiation interaction potential. In an attempt to improve the shielding ability of CRT screen glass, Alrowaili et al.¹⁴ produced glass ceramic samples from a combination of TV screen glass (S-TV) and TiO_2 . They investigated the role of TiO_2 content, which varied between 0 wt.% and 10 wt.%, on the hardness, density, microstructure, and radiation shielding abilities of the samples. The results showed that the glass hardness improved with TiO_2 content. In addition, the optimal values of density, surface compactness, charged particle (carbon ions, alpha particles, protons, and electrons), thermal neutron, and fast neutron interaction cross-sections were obtained for samples containing 10 wt.% TiO_2 , confirming that the addition of TiO_2 is a successful method for improving the radiation absorption of S-TV glass. However, radiation of different qualities and relative biological efficacy interacts with matter differently. Consequently, the shielding behaviour of a medium can differ for different radiation qualities. Gamma photons are a widely used radiation type; their high penetrability is one reason that many shielding designs are targeted at photons (gamma rays and x-rays). It is hence crucial that the gamma-photon shielding ability of a medium be ascertained before it can be fully described as a good radiation shield. Since the charged radiation and neutron penetration parameters were obtained in our previous study, the present study helps to provide additional data on the scope of shielding that can be achieved with the use of TiO_2 -doped S-TV to absorb gamma photons.

In this paper, the gamma radiation shielding properties of S-TV/ TiX glasses were investigated at different photon energies using data from FLUKA simulations and the XCOM library. This study attempts to provide alternative and effective gamma radiation shielding glasses as well as a safe route

for recycling of CRT screen glasses. The study is therefore justified and significant from the perspective of radiation safety and environmental conservation.

Methodology

Three samples of S-TV doped with TiO₂ were prepared using cold isostatic pressing. The samples were designated as S-TV, S-TV/Ti10, and S-TV/Ti20 for TiO₂ concentrations of 0 wt.%, 10 wt.%, and 20 wt.%, respectively. The screen glass was separated from the cone part of the CRT of a discarded TV through standard laboratory procedures. The glass was then crushed with the aid of a vibratory mill operated at 3000 rpm for 1200 s. The resulting powder was thoroughly mixed with the required concentration of TiO₂ for about 1800 s, after which a consistent powder was obtained. The sample containing TiO₂ appeared greenish in colour. The three mixtures were pressureless sintered at 1073 K for 3600 s. After the heating process, the powder samples were further crushed, and cold isostatic pressing was used to obtain bulk samples. Pressure of 250 MPa was applied to densify the samples in steel moulds. Details of the preparatory routes were described in our previous publication.¹⁴ The sample density was measured, and the proportion of chemical oxides present in the S-TV/TiX samples was determined using x-ray fluorescence (XRF).

Gamma radiation transmission data for the samples were obtained from FLUKA simulations. Using the narrow-beam transmission setup in the FLUKA environment as shown in Fig. 1, the intensity of incident photons and photons transmitted through a thin glass sample were obtained and used to evaluate the mass (μ/ρ) and linear (μ) attenuation coefficients of the samples for photon energies within the range of 15 keV to 15 MeV range. To validate the accuracy of the narrow-beam geometry employed, the mass attenuation coefficients of the samples were also computed using the XCOM database. In both cases, the chemical composition of the glasses as obtained from the XRF analysis is tabulated in

Table SI. The bulk densities of the samples as obtained from laboratory measurements are also given in Table SI. Other photon interaction parameters, including the HVL, mean free path (λ), effective atomic number (Z_{eff}), electron density (N_{eff}), specific gamma constant (Γ), dose rate ((D_r) , equivalent atomic number (Z_{eq}), exposure (EBF), and energy absorption (EABF) buildup factor were calculated from the mass attenuation coefficient data using standard expressions and procedures highlighted in the literature,¹⁶⁻²¹ some of which are shown in Table II. In these equations, f_i is the weight fraction of each element in the glass composition having atomic number Z_i , mass number A_i , mass attenuation coefficient $\left(\frac{\mu}{\rho}\right)_i$, and mass energy absorption coefficient $\left(\frac{\mu_{\text{en}}}{\rho}\right)_i$. The mass attenuation coefficients of the prepared glasses were obtained from the glass thickness used in the simulation process, the incident photon flux (N_o), and transmitted flux (N) data from the simulations as seen in Eq. 1. XCOM used the summation rule in Eq. 2 in the table for estimating mass attenuation coefficients of the glasses.

Results and Discussion

Mass and Linear Attenuation Coefficient

The mass and linear attenuation coefficients are fundamental quantities that are often used to quantify the amount of gamma radiation transmitted through a barrier from a given incident beam. The quantities depend on the energy of photons and barrier characteristics such as density or thickness (for μ/ρ) and the nature and amount of chemical species present in the medium of interaction or barrier. The values of the mass (μ/ρ) attenuation coefficients of the S-TV/TiX glasses obtained from data using the XCOM library and FLUKA simulations are displayed for different gamma-photon energies in Table SIII. Using Eq. 1, the relative differences (RD (in %)) between the two sets of μ/ρ

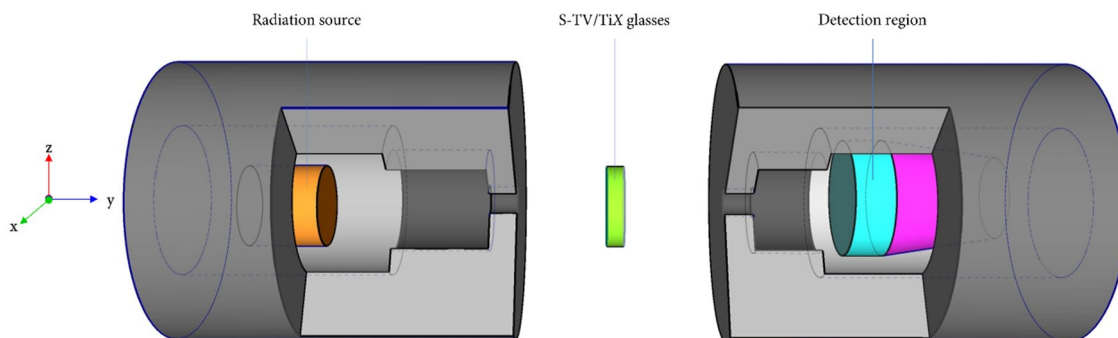


Fig. 1 FLUKA simulation setup used for evaluating the gamma-ray transmission capacities of the synthesized S-TV/TiX glasses.

were estimated, and the obtained absolute values are given in Table SIII as well.

$$\text{RD}(\%) = \frac{(\mu/\rho)^{\text{XCOM}} - (\mu/\rho)^{\text{FLUKA}}}{(\mu/\rho)^{\text{XCOM}}} \times 100 \quad (1)$$

The RD values fluctuate between 0.047 and 0.941%. These represent a strong agreement between the μ/ρ values. The marginal differences also confirm the validity of the simulation setup in producing narrow-beam transmission through a thin glass sample. The values of μ/ρ in the table showed strong energy variations and differed from one glass sample to another. The μ/ρ values are in the range of 0.02442–12.57505 cm²/g, 0.02438–13.54632 cm²/g, and 0.02434–14.50959 cm²/g for S-TV, S-TV/Ti10, and S-TV/Ti20, respectively. Also, the computed linear attenuation coefficients (μ) range from 0.06165 cm⁻¹ to 31.75199 cm⁻¹, 0.06207 cm⁻¹ to 34.48893 cm⁻¹, and 0.06048 cm⁻¹ to 36.05632 cm⁻¹ in the samples with 0 wt.%, 10 wt.%, and 20 wt.% TiO₂. The energy variations in the values of μ and μ/ρ are depicted in Fig. 2a and b, respectively. The magnitudes of the attenuation coefficients of the glasses decrease with gamma-ray energy. Generally, as the energy of gamma radiation increases, the photon interaction probability decreases at rates dictated by the energy dependence of the various interaction modes, including coherent and incoherent scattering, the photoelectric effect, and pair production absorption.^{14,15,21} The implication of this is that the glasses can absorb more photon intensities at lower energies than at higher energies. Looking at the μ and μ/ρ values, it is clear that the attenuation coefficients vary as the glass density and TiO₂ content vary. At 15 keV, the values for μ and μ/ρ follow the order S-TV < S-TV/Ti10 < S-TV/Ti20. However, for the rest of the energy spectrum, the trend is reversed. The addition of TiO₂ appears to enhance the shielding ability of S-TV for 15 keV (and perhaps lower energy) gamma-ray photons. The introduction of TiO₂ resulted in the reduction of other oxides in the S-TV structure, as seen in Table SI. The introduction of TiO₂ and subsequent increase, in addition to the proximity of 15 keV to the absorption edges of heavy metals such as Sr (16.1 keV) and Zr (17.997 keV), is responsible for the trend in μ and μ/ρ at 0.015 MeV and perhaps lower energies. At higher energies, the decrease in the concentration of heavy metal oxides such as BaO, SrO, ZrO₂, and Sb₂O₃ affects the reduction of the total photon interaction probability as TiO₂ increases in concentration. The maximum decrease in the value of μ/ρ when 10 wt.% TiO₂ was introduced into the S-TV structure was 5.58% at 50 keV. Beyond this point, the decrease in μ/ρ of S-TV/Ti10 with respect to S-TV decreased to almost zero as the energy increased. For S-TV/Ti20, the maximum and minimum decrease in the values of μ/ρ were 11.18% and 0.33% at 50 keV and 15 MeV, respectively. The photoelectric effect

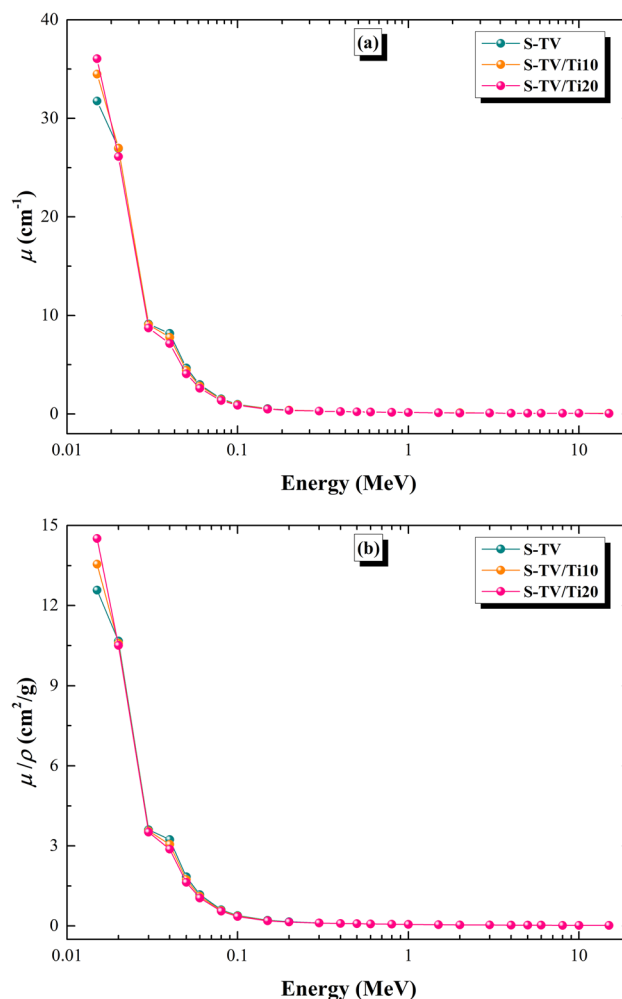


Fig. 2 (a) Linear attenuation coefficient and (b) mass attenuation coefficient of the synthesized S-TV/TiX glasses with different photon energies.

(PE) is more sensitive to changes in the chemical definition of a medium than other photon interaction processes. Therefore, the greatest variation is observed in the keV energy range where PE interaction is significant. The density of the glasses does not appear to influence the trends in the values of the attenuation coefficients, unlike the chemical composition.

Half-Value Layer

The HVL is an important parameter for assessing the gamma-ray absorption efficiency of a medium in terms of thickness. Using the HVL, the thickness required to absorb different proportions of the incident beam can be calculated. For example, the first HVL is the thickness of a shield that reduces an incident beam by 50%; the second HVL reduces the beam to 25%. Figure 3 displays the energy variations in the HVLs of the S-TV/TiX glasses for different

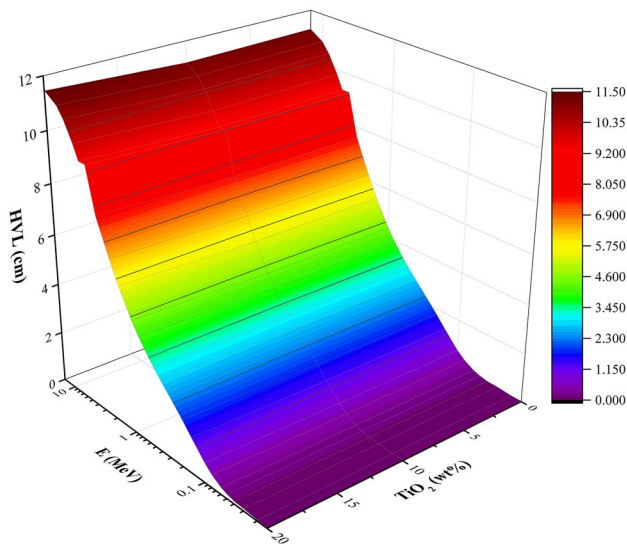


Fig. 3 Half-value layer (HVL) with respect to the concentration of TiO_2 and a function of photon energy in the synthesized S-TV/TiX glasses.

TiO_2 concentrations. For the present S-TV/TiX samples, the values of the HVL are greatest at 15 MeV, with values of 11.24241 cm, 11.16704 cm, and 11.46075 cm for the samples with 0 wt.%, 10 wt.%, and 20 wt.% TiO_2 , respectively. Conversely, minimum values of 0.02183 cm, 0.02010 cm, and 0.01922 cm for S-TV, S-TV/Ti10, and S-TV/Ti20, respectively, were obtained for 15 keV photons. Generally, the HVLs increase with the increase in TiO_2 content and photon energy due to the decrease in the probability of photon absorption processes such as the photoelectric effect and Compton scattering. An increase in TiO_2 content increases the thickness required for the glasses to attenuate photons for most of the energy spectrum considered.

Mean Free Path

The mean free path (MFP, λ) is another value that can be used to characterize the interaction of gamma rays with matter. It describes the mean path length of photons in a medium between interactions. Materials with low photon transmission are characterized by lower λ . Qualitatively, λ behaves similarly to the HVL with respect to gamma energy. The MFPs of the S-TV/TiX glasses have the highest values at 15 MeV while their lowest values are at 0.015 MeV. The MFPs of S-TV/TiX glasses vary from 0.03149 cm to 16.21937 cm for S-TV, from 0.02899 cm to 16.11063 cm for S-TV/Ti10, and from 0.02773 cm to 16.53437 cm for S-TV/Ti20. Figure 4 compares the MFPs of the synthesized glasses with those of different shielding materials. In Fig. 4a, the MFPs of the S-TV/TiX glasses are higher than those of the RS 323 G19 commercial glass shield^{22,23} for 0.2 MeV, 0.662

MeV, and 1.25 MeV photons, indicating that the S-TV/TiX glasses transmit more photons relative to the commercial glass. However, the prepared S-TV/TiX showed superior gamma radiation shielding ability relative to RS 253 and RS 253 G18^{22,23} due to the lower MFP for 0.2 MeV photons. The present glasses have comparable shielding ability to the RS 253 and RS 253 G18 glasses for 0.662 MeV to 1.25 MeV photons (see Fig. 4a). Figure 4b shows that the MFPs of the S-TV/TiX glasses are higher than those of the SLGC-E5.²⁴ It also shows that they are comparable to those of TLP-A²⁵ and BBLNi6²⁶ for gamma energies less than 6 MeV and higher (lower) than those of TLP-A (BBLNi6) at greater energies. Compared to different concrete samples,²⁷ the MFPs of the S-TV/TiX glasses are smaller than those of ordinary concrete (OC), and they are higher than the MFPs of ilmenite-limonite (IL), basalt-magnetite (BM), and ilmenite (IN) concrete, in particular between 1 MeV and 10 MeV (see Fig. 4c). There is no remarkable difference between the MFPs of the S-TV/TiX glasses and the MFPs of hematite-serpentine concrete (HS). The glasses can thus shield against photons with nearly equal efficiency as HS but better than OC. Finally, in Fig. 4d, it is clear that the MFPs of P2²⁸ and guanine²⁹ are higher than those of the S-TV/TiX glasses. The differences in the shielding ability of the different materials compared with the present glasses can be attributed mainly to the variations in the chemical composition. The photon interaction of a medium is the sum total of the interactions of all the elements contained in the medium. Therefore, materials containing higher concentrations of heavier atoms have higher cross-sections for photon interaction and lower MFPs, and are thus better shields. For example, the presence of Pb in RS 323 G19 explains why it appears to be a better shield than the S-TV/TiX glasses. However, the environmental concerns as regards Pb are a drawback for the superior RS 323 G19 glass shields. Furthermore, the fact that the S-TV/TiX glasses are derived from waste glass makes them superior to the other glasses with better shielding capacity from an economic and environmental perspective. It can be concluded that the present S-TV/TiX glasses have better photon shielding abilities and advantages than some well-known shielding materials, such as ordinary concrete and commercial glass shields, especially at low photon energies.

Effective Atomic Number and Electron Density

In most of the interaction processes between gamma photons and matter, photon absorption or energy deposition processes occur between photons and electrons. The effective number of electrons or electrons per mass present in matter can be used to describe the shielding ability or energy absorption capacity of a medium. The effective atomic number Z_{eff} and electron density N_{eff} are used to describe the effective number of electrons or

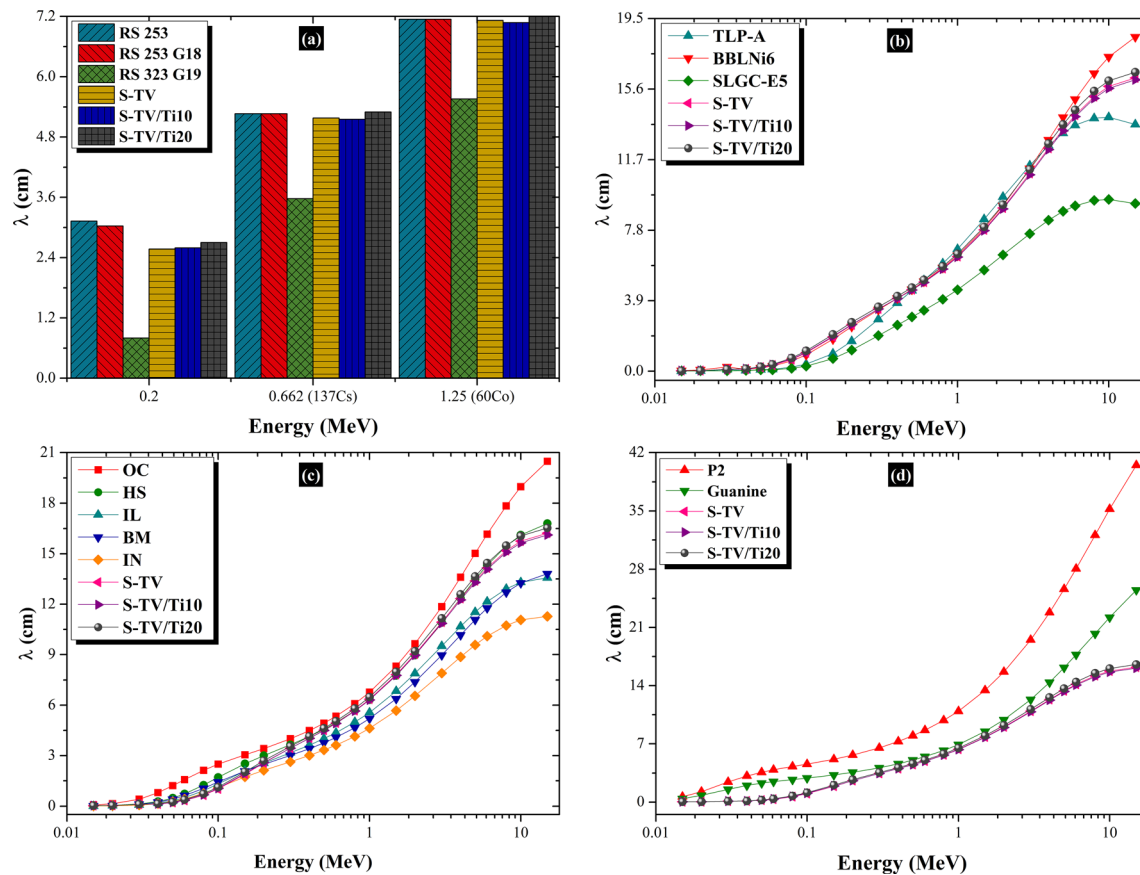


Fig. 4 Comparison of mean free path (λ) values of S-TV/TiX glasses with those in (a) commercially available SCHOTT radiation shielding glasses (data from Refs. 22 and 23), (b) standard radiation shielding

glasses (data from Refs. 23–26), (c) concrete samples (data from Ref. 27), and (d) various materials (data from Refs. 28 and 29).

electrons per unit mass available for photon interactions, respectively. The Z_{eff} has values between 11.55 and 34.77 for S-TV, 11.65 and 33.54 for S-TV/Ti10, and 11.75 and 32.26 for S-TV/Ti20. The corresponding values for N_{eff} are 2.93×10^{23} and 8.83×10^{23} electrons/g, 2.92×10^{23} and 8.42×10^{23} electrons/g, and 2.92×10^{23} and 8.01×10^{23} electrons/g. The changes in the values of Z_{eff} and N_{eff} are demonstrated in Fig. 5a and b, respectively. The fluctuations of both quantities with energy are similar, as expected. The maximum and minimum values of both Z_{eff} and N_{eff} are obtained at 40 keV and 1500 MeV, respectively. The high values of both parameters at 40 keV are the result of the strong photoelectric interaction of the K-electrons of the Ba atoms. The reduction of Z_{eff} and N_{eff} at this energy is due to the reduction in the weight fraction of Ba in the glass samples (as seen in Table SI). Compton scattering of photons is responsible for the lowest values of Z_{eff} and N_{eff} at 1.5 MeV. The values of Z_{eff} and N_{eff} are generally in the order S-TV > S-TV/Ti10 > S-TV/Ti20. This shows that the glass sample with lower TiO₂ content presents more electron interactions and hence absorbs more photons.

Mass Energy Absorption Coefficient, Specific Gamma Constant, and Dose Rate

The mass energy absorption coefficient (MEAC), specific gamma constant (Γ), and dose rate (D_r) are quantities that specify how much energy is absorbed from photons. They are dependent on the nature of the material and the gamma energy. The MEACs of the S-TV/TiX glasses are in the range 0.0177–11.7580 cm²/g, 0.0177–12.6327 cm²/g, and 0.0176–13.5007 cm²/g for S-TV, S-TV/Ti10, and S-TV/Ti20, respectively. The MEACs of the S-TV/TiX glasses decrease with the enhancement of photon energy (see Fig. 6a), with the lowest and highest values obtained at 10 MeV and 0.015 MeV, respectively. The behaviour of MEAC with respect to energy is attributed to the effects of the various interaction modes in a similar way as the mass attenuation coefficient. Aside from energies below 50 keV, the energy deposited by photons in the glasses is nearly equal for the photon energies considered.

The maximum and minimum values of Γ for the S-TV/TiX glasses were observed at 15 MeV and 0.2 MeV, respectively, as depicted in Fig. 6b. The Γ values of the S-TV/

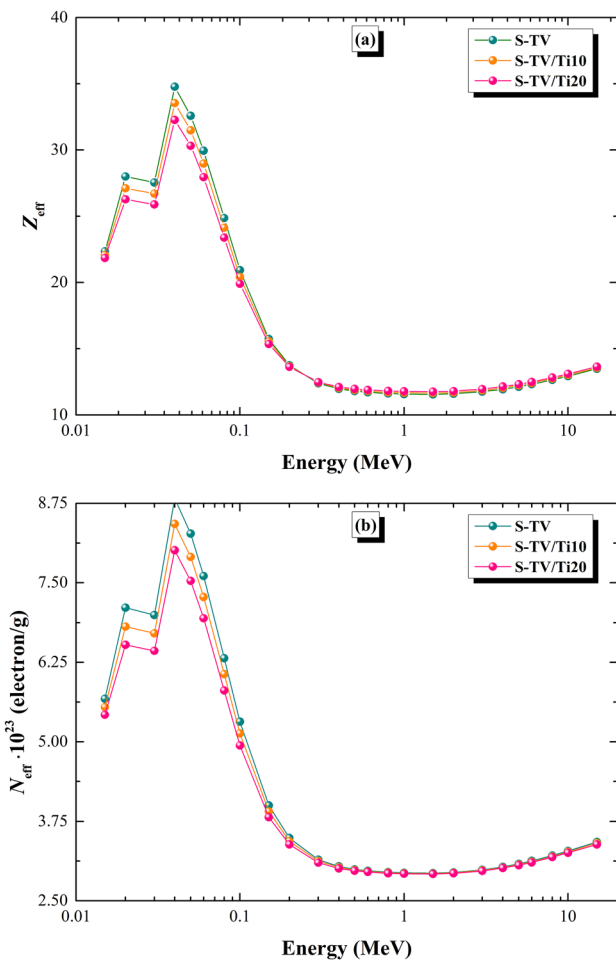


Fig. 5 (a) Effective atomic number and (b) effective electron density of the synthesized S-TV/TiX glasses, with different photon energies.

TiX glasses are in the range of 6.91812–175.09345 Rm^2/Ci h, 6.66150–175.01183 Rm^2/Ci h, and 6.40394–174.90401 Rm^2/Ci h in the samples with 0 wt.%, 10 wt.%, and 20 wt.% TiO_2 , respectively. The decrease in photon interactions with increased energy is responsible for the initial drop in values and increase in photon energy; the ionization effect due to pair production is responsible for the later increase in the values of Γ .

The gamma dose rate (D_r) is directly proportional to the MEAC, and consequently the changes in the values of D_r are influenced by the two former quantities. In Fig. 7, the absorbed dose rates in S-TV/TiX glasses with thickness of 1 mm, 5 mm, 10 mm, and 15 mm are plotted against energy. The D_r values are lower for thicker glasses due to the geometric and exponential attenuation of photons, which increases with geometric thickness and the number of mean free paths of the glass barriers, respectively. Therefore, doses for 1-mm-thick glasses are highest, while those for 15-mm-thick glasses are lowest. Because the MEAC and Γ are almost equal at the same energy, the dose rates are

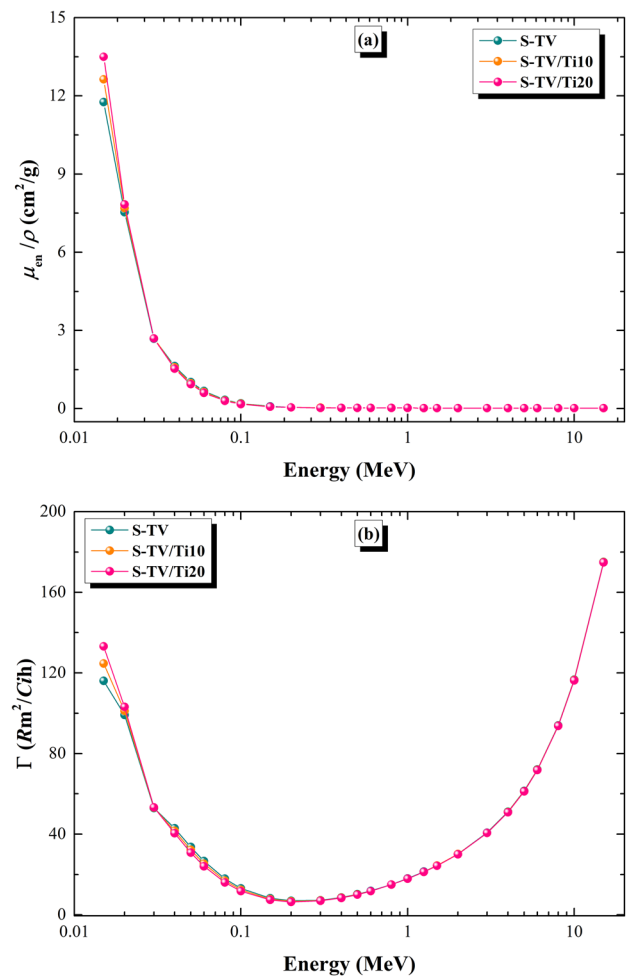


Fig. 6 (a) Mass energy-absorption coefficient and (b) specific gamma-ray constant of the synthesized S-TV/TiX glasses, with different photon energies.

almost equal for equal glass thickness and photon energy at energies above 50 keV.

Equivalent Atomic Number and Buildup Factors

In the broad-beam transmission of gamma rays through thick absorbers, photons are scattered multiple times depending on the thickness of the absorber. When applied to a broad-beam situation, the narrow-beam approximation overestimates the attenuation parameters. The photon buildup factors (BFs) are calculated and used to correct the degree of attenuation to fit the broad-beam scenarios. There are many BFs depending on the gamma-photon response quantity of interest. The exposure buildup factor (EBF) and the energy absorption BF (EABF) are two well-known BFs when the response functions of interest are the exposure and energy absorbed, respectively. The evaluation of the BFs through the GP fitting procedure requires the calculation of the

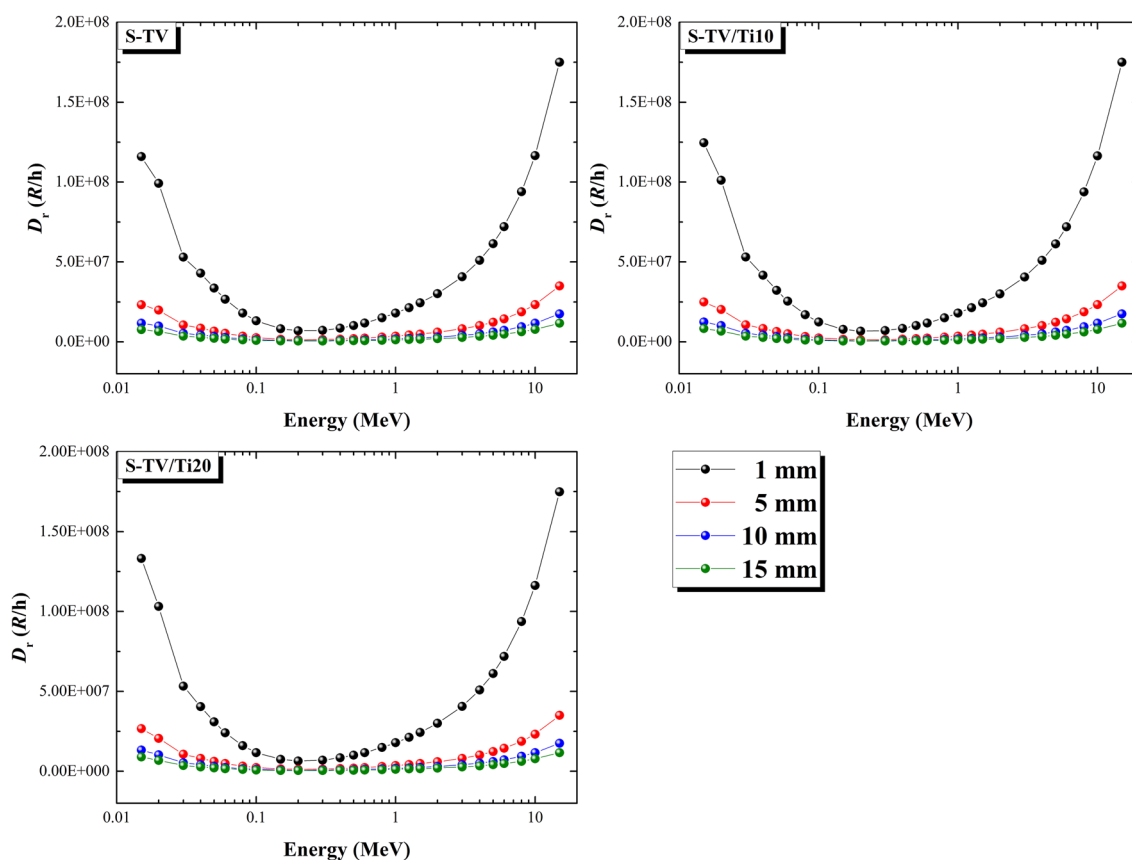


Fig. 7 Gamma dose rate at different photon energy levels for the synthesized S-TV/TiX glasses.

equivalent atomic number (Z_{eq}) of a composite material, which gives the atomic number of the chemical element that has similar photon scattering properties.^{16,18,30} The estimated values of Z_{eq} for the S-TV/TiX glasses are plotted against the energy of photons in Fig. 8. The highest values for each of the glasses obtained at 0.8 MeV are 18.65, 18.70, and 18.75 for S-TV samples doped with 0 wt.%, 10 wt.%, and 20 wt.% TiO₂, respectively. On the other hand, the lowest values of 14.04, 14.45, and 14.84 for S-TV, S-TV/Ti10, and S-TV/Ti20, respectively, were obtained at 0.015 MeV. At 1.5 MeV, the Z_{eq} values of the glasses are almost equal; below this energy, the values of Z_{eq} vary in the order of S-TV/Ti20 > S-TV/Ti10 > S-TV. This order is reversed at energies above 1.5 MeV (see Fig. 8). The changes in the values and trend of Z_{eq} indicate that the photon scattering capacity of the glasses depends on the photon energy and chemical content of the glasses.

The estimated EBF and EABF are presented in Figs. 9 and 10, respectively, as a function of energy and TiO₂ concentration for 1 mfp, 5 mfp, 10 mfp, 20 mfp, 30 mfp, and 40 mfp glass depths. The spectra of the BFs have similar features. Firstly, the values of the BFs increase with glass depth. Therefore, the lowest BF values were obtained at

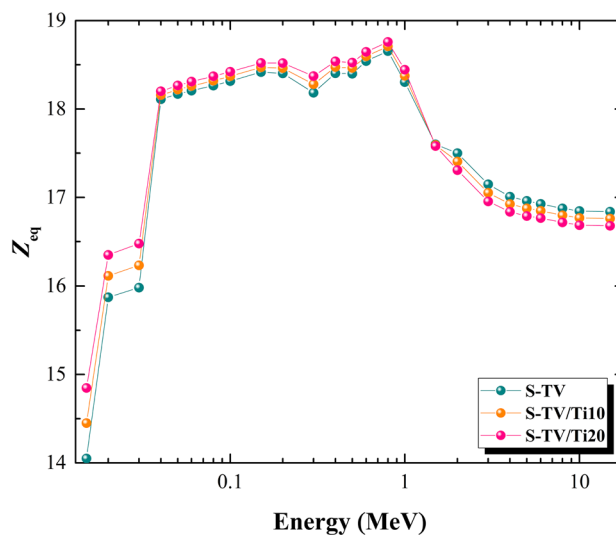


Fig. 8 Equivalent atomic number (Z_{eq}) with the photon energy for the synthesized S-TV/TiX glasses.

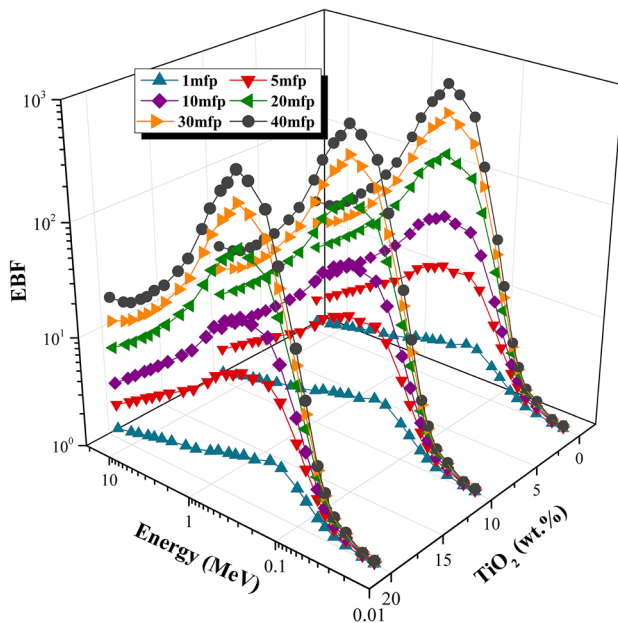


Fig. 9 Exposure buildup factor (EBF) with the photon energy for the synthesized S-TV/TiX glasses.

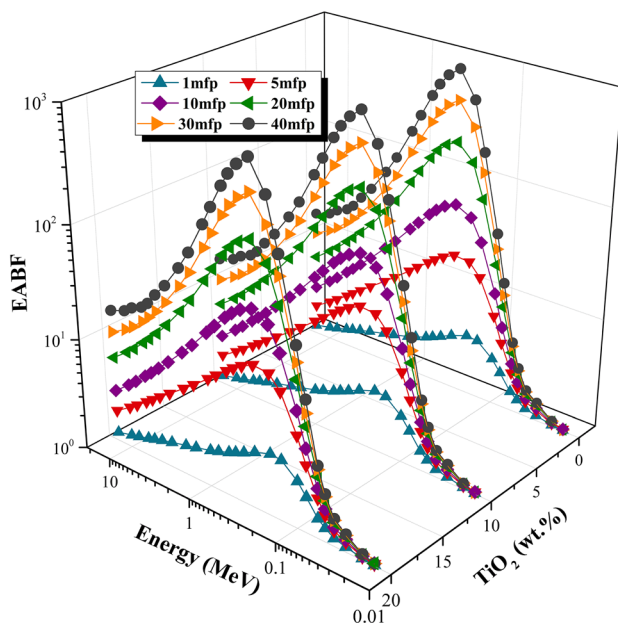


Fig. 10 Energy absorption buildup factor (EABF) with the photon energy for the synthesized S-TV/TiX glasses.

1 mfp, while the highest were obtained for 40 mfp thick glasses. This can be attributed to the greater number of photon collisions in thicker glasses. Secondly, the spectrum of each BF can be divided into three regions: the high, the low, and intermediate regions. The low region is where the magnitudes of the BFs are lowest. This coincides with the region below 0.5 MeV. The low BF values are attributed

to the photoelectric absorption of photons, which prevents buildup. The increase in the values of the BFs in this region with respect to energy is due to the increased probability of the Compton scattering of gamma rays. The peak of the BFs is the point where the scattering of photons is greatest (high region). In the intermediate region, the BFs are lower than those in the Compton scattering-dominated region but higher than those where the photoelectric effect is significant. The pair production absorption process is dominant in this region. Although this absorption mode removes incident photons completely, it produces secondary photons, which are further scattered, especially in thicker glasses. Finally, the glasses with lower TiO₂ content had higher BFs. It can thus be concluded that doping with TiO₂ prevents photon buildup in the S-TV glasses.

Conclusion

Cold isostatic pressing was used to prepare TV screen glass (S-TV) doped with 0 wt.%, 10 wt.%, and 20 wt.% TiO₂. The gamma radiation shielding properties of S-TV/TiX glasses were investigated at different photon energies using data from FLUKA simulations and the XCOM library. The gamma radiation attenuation coefficients from FLUKA simulations agreed well with those computed using the XCOM database. The μ/ρ values were in the range of 0.02442–12.57505 cm²/g, 0.02438–13.54632 cm²/g, and 0.02434–14.50959 cm²/g for S-TV, S-TV/Ti10, and S-TV/Ti20, respectively. Also, the computed linear attenuation coefficients (μ) were between 0.06165 and 31.75199 cm⁻¹, 0.06207 and 34.48893 cm⁻¹, and 0.06048 and 36.05632 cm⁻¹ in the samples with 0 wt.%, 10 wt.%, and 20 wt.% TiO₂. The density of the glasses did not appear to influence the trends in the values of the attenuation coefficients, unlike the chemical composition. The Z_{eff} values were between 11.55 and 34.77 for S-TV, 11.65 and 33.54 for S-TV/Ti10, and 11.75 and 32.26 for S-TV/Ti20. The corresponding values for N_{eff} were 2.93×10^{23} and 8.83×10^{23} electrons/g, 2.92×10^{23} and 8.42×10^{23} electrons/g, and 2.92×10^{23} and 8.01×10^{23} electrons/g. The values of Z_{eff} and N_{eff} were generally in the order S-TV > S-TV/Ti10 > S-TV/Ti20, which shows that the glass sample with lower TiO₂ content presents more electron interactions and hence absorbs more photons. The MEACs of the S-TV/TiX glasses were in the range of 0.0177–11.7580 cm²/g, 0.0177–12.6327 cm²/g, and 0.0176–13.5007 cm²/g for S-TV, S-TV/Ti10, and S-TV/Ti20, respectively. The Γ values of the S-TV/TiX glasses were in the range of 6.91812–175.09345 Rm²/Ci h, 6.66150–175.01183 Rm²/Ci h, and 6.40394–174.90401 Rm²/Ci h in the samples with 0 wt.%, 10 wt.%, and 20 wt.% TiO₂, respectively. The values of Z_{eq} varied in the

order of S-TV/Ti20 > S-TV/T10 > S-TV. This order was reversed at energies above 1.5 MeV because the glasses with lower TiO₂ content had higher BFs. Although previous studies have highlighted a significant improvement in the gamma attenuation capacity of different glass matrices^{1,3,6–8} when doped with TiO₂, its influence on the gamma-photon absorption capacity of S-TV varied with energy. The most significant improvement in the gamma attenuation parameters was observed in the low-energy (keV) region. It was also observed in this study that doping of S-TV with TiO₂ suppressed the buildup of photons in broad-beam transmission scenarios. In comparison with some standard radiation shields, TiO₂-doped S-TV glasses have better gamma-absorption capacity and are therefore suitable for gamma-shielding applications, especially for low (keV) energies.

Supplementary Information The online version contains supplementary material available at <https://doi.org/10.1007/s11664-024-10936-x>.

Acknowledgments The authors express their gratitude to Princess Nourah bint Abdulrahman University Researchers Supporting Project number (PNURSP2024R26), Princess Nourah bint Abdulrahman University, Riyadh, Saudi Arabia.

Author contributions All the authors have accepted full responsibility for the content of this manuscript and have given their approval to its submission.

Data availability All data associated with this study are included in the manuscript and supplementary information file.

Conflict of interest The authors declare that they have no conflict of interest.

References

- B. Albarzan, M.Y. Hanfi, A.H. Almuqrin, M.I. Sayyed, H.M. Alsafi, and K.A. Mahmoud, The influence of titanium dioxide on silicate-based glasses: an evaluation of the mechanical and radiation shielding properties. *Materials* 14, 3414 (2021).
- I. Kebaili, I. Boukhris, M.I. Sayyed, B. Tonguc, and M.S. Al-Buriahi, Effect of TiO₂/V₂O₅ substitution on the optical and radiation shielding properties of alkali borate glasses: A Monte Carlo investigation. *Ceram. Int.* 46, 25671 (2020).
- G.P. Singh, J. Singh, P. Kaur, T. Singh, R. Kaur, S. Kaur, and D.P. Singh, Impact of TiO₂ on radiation shielding competencies and structural, physical and optical properties of CeO₂-PbO-B₂O₃ glasses. *J. Alloys Compd.* 885, 160939 (2021).
- G. Hussan, S. Khan, R. Ahmad, A. Farooq, and M.Z. Anwar, Effect of WO₃ on the radiation shielding ability of TeO₂-TiO₂-WO₃ glass system. *Radiochim. Acta* 111(5), 401 (2023).
- H. Karami, V. Zanganeh, and M. Ahmadi, Study nuclear radiation shielding, mechanical and Acoustical properties of TeO₂-Na₂O-BaO-TiO₂ alloyed glasses. *Radiat. Phys. Chem.* 208, 110917 (2023).
- A. Arvaneh, A. Asadi, and S.A. Hosseini, Sensitivity analysis of gamma-ray shielding characteristics to the TiO₂ concentration in the Bi₂O₃-ZnO-Pb₃O₄-Al₂O₃ glass sample based on the Monte Carlo method. *Prog. Nucl. Energy* 156, 104539 (2023).
- H. Es-soufi, H. Bih, M.I. Sayyed, and L. Bih, Impact of TiO₂ on physical, optical, and radiation shielding properties of tungsten-based glasses. *Optik* 272, 170400 (2023).
- R. Rahmat, N. Halima, H. Heryanto, E. Sesa, and D. Tahir, Improvement X-ray radiation shield characteristics of composite cement/ Titanium dioxide (TiO₂)/Barium carbonate (BaCO₃): Stability crystal structure and chemical bonding. *Radiat. Phys. Chem.* 204, 110634 (2023).
- J. Bawab, J. Khatib, H. El-Hassan, L. Assi, and M.S. Kirgiz, Properties of cement-based materials containing cathode-ray tube (CRT) glass waste as fine aggregates—A review. *Sustainability* 13(20), 11529 (2021).
- R.B. Malidarre and I. Akkurt, A comprehensive study on the charged-uncharged particle shielding features of (70-x) CRT-30K20-x BaO glass system. *J. Aust. Ceram. Soc.* 58(3), 841 (2022).
- R. Kurtuluş, T. Kavas, O. Agar, M.F. Turhan, M.R. Kaçal, I. Dursun, and F. Akman, Study on recycled Er-incorporated waste CRT glasses for photon and neutron shielding. *Ceram. Int.* 47(18), 26335 (2021).
- M.S. Al-Buriahi, T. Kavas, E. Kavaz, R. Kurtulus, and I.O. Olarinoye, Recycling potential of cathode ray tubes (CRTs) waste glasses based on Bi₂O₃ addition strategies. *Waste Manage.* 148, 43 (2022).
- M.I. Sayyed, N. Almousa, and M. Elsafi, Green conversion of the hazardous cathode ray tube and red mud into radiation shielding concrete. *Materials* 15(15), 5316 (2022).
- Z.A. Alrowaili, J.S. Alzahrani, M. Kirkbinar, E. İbrahimoglu, F. Çalışkan, I.O. Olarinoye, and M.S. Al-Buriahi, Role of TiO₂ addition on recycling of TV screen waste glasses: Experimental and theoretical studies on structure and radiation attenuation properties. *Ceram. Int.* 49(17), 28022 (2023).
- M.S. Al-Buriahi, J.S. Alzahrani, Z.A. Alrowaili, I.O. Olarinoye, and C. Sriwunkum, Recycling of waste cathode-ray tube glasses as building materials for shielding structures in medical and nuclear facilities. *Constr. Build. Mater.* 376, 131029 (2023).
- I.O. Olarinoye, R.I. Odiaga, and S. Paul, EXABCal: A program for calculating photon exposure and energy absorption buildup factors. *Heliyon* 5(7), e02017 (2019).
- Y.S. Rammah, I.O. Olarinoye, F.I. El-Agawany, K.A. Mahmoud, I. Akkurt, and E. Yousef, Evaluation of radiation shielding capacity of vanadium-tellurite-antimonite semiconducting glasses. *Opt. Mater.* 114, 110897 (2021).
- E. Şakar, Ö.F. Özpolat, B. Alım, M.I. Sayyed, and M. Kurudirek, Phy-X/PSD: development of a user-friendly online software for calculation of parameters relevant to radiation shielding and dosimetry. *Radiat. Phys. Chem.* 166, 108496 (2020).
- E. Kavaz, M.C. Ersundu, A.E. Ersundu, and H.O. Tekin, Synthesis and characterization of newly developed phosphate-based glasses through experimental gamma-ray and neutron spectroscopy methods: Transmission and dose rates. *Ceram. Int.* 48(10), 13842 (2022).
- G.B. Cengiz and İ Çağlar, Assessment of mass attenuation coefficient, effective atomic number and electron density of some aluminum alloys. *Caucasian J. Sci.* 7(2), 109 (2020).
- I.O. Olarinoye, S. Alomairy, C. Sriwunkum, and M.S. Al-Buriahi, Effect of Ag₂O/V₂O₅ substitution on the radiation shielding ability of tellurite glass system via XCOM approach and FLUKA simulations. *Phys. Script.* 96(6), 065308 (2021).
- Speid, B. (1991). Radiation-shielding glasses providing safety against electrical discharge and being resistant to discoloration. Google Patents. <https://patents.google.com/patent/US5073524A/en> Accessed 04 June 2023

23. <https://www.schott.com/en-ca/products/radiation-shielding-glasses/product-variants?tab=rs-glass-series> Accessed 04 June 2023.
24. M.S. Al-Buriahi, D.K. Gaikwad, H.H. Hegazy, C. Sriwunkum, and H. Algarni, Newly developed glasses containing Si/Cd/Li/Gd and their high performance for radiation applications: role of Er₂O₃. *J. Mater. Sci. Mater. Electron.* 32, 9440 (2021).
25. A. Alalawi, C. Eke, N.J. Alzahrani, S. Alomairy, O. Alsalmi, C. Sriwunkum, Z.A. Alrowaili, and M.S. Al-Buriahi, Attenuation properties and radiation protection efficiency of Tb₂O₃-La₂O₃-P₂O₅ glass system. *J. Aust. Ceram. Soc.* 58, 511 (2022).
26. M.S. Al-Buriahi, A.S. Abohaswa, H.O. Tekin, C. Sriwunkum, F.I. El-Agawany, T. Nutaro, E. Kavaz, and Y.S. Rammah, Structure, optical, gamma-ray and neutron shielding properties of NiO doped B₂O₃-BaCO₃-Li₂O₃ glass systems. *Ceram. Int.* 46(2), 1711 (2020).
27. I.I. Bashter, Calculation of radiation attenuation coefficients for shielding concretes. *Ann. Nucl. Energy* 24(17), 1389 (1997).
28. M.S. Al-Buriahi, C. Eke, S. Alomairy, A. Yildirim, H.I. Alsaedy, and C. Sriwunkum, Radiation attenuation properties of some commercial polymers for advanced shielding applications at low energies. *Polym. Adv. Technol.* 32, 2386 (2021).
29. M.S. Al-Buriahi, C. Sriwunkum, and I. Boukhris, X- and gamma-rays attenuation properties of DNA nucleobases by using FLUKA simulation code. *Eur. Phys. J. Plus* 136, 776 (2021).
30. I.O. Olarinoye, F.I. El-Agawany, A. El-Adawy, and Y.S. Rammah, Mechanical features, alpha particles, photon, proton, and neutron interaction parameters of TeO₂-V₂O₃-MoO₃ semiconductor glasses. *Ceram. Int.* 46(14), 23134 (2020).

Publisher's Note Springer Nature remains neutral with regard to jurisdictional claims in published maps and institutional affiliations.

Springer Nature or its licensor (e.g. a society or other partner) holds exclusive rights to this article under a publishing agreement with the author(s) or other rightsholder(s); author self-archiving of the accepted manuscript version of this article is solely governed by the terms of such publishing agreement and applicable law.